Energy 252 (2022) 124043

Contents lists available at ScienceDirect

Energy

journal homepage: www.elsevier.com/locate/energy

Fluctuation of fracturing curves indicates in-situ brittleness and reservoir fracturing characteristics in unconventional energy exploitation

Fuqiang Sun [a, b], Shuheng Du [a, b], Ya-Pu Zhao [a, b, *]

[a] State Key Laboratory of Nonlinear Mechanics, Institute of Mechanics, Chinese Academy of Sciences, Beijing, 100190, China
[b] School of Engineering Science, University of Chinese Academy of Sciences, Beijing, 100049, China

ARTICLE INFO

Article history:
Received 30 November 2021
Received in revised form
15 March 2022
Accepted 14 April 2022
Available online 16 April 2022

Keywords:
Brittleness index
Data-driven optimization
Fracturing curve
Micro-seismic data
Unconventional reservoir
Ashby plots

ABSTRACT

Reservoir brittleness is a key index to evaluate the fracability and to predict the fracturing characteristics in unconventional energy exploitation. Traditional brittleness indices could only be derived from laboratory experiments, which are far from the field conditions and may lead to deviations. In this paper, a fracturing-curve based in-situ brittleness evaluation method is proposed and the in-situ brittleness of Woodford Shale is derived under field stress and temperature conditions. Based on the analysis of real-time micro-seismic data, it is confirmed that the real-time fracturing characteristics can be known by observing the fluctuations in the fracturing curves. Results showed that the in-situ brittleness is much lower than that derived in laboratory experiments. About 78% of micro-seismic events happen at the extreme value and the fastest fluctuation of the fracturing curve. These provide guidance for accurate formulation and real-time optimization of exploitation scheme.

1. Introduction

Hydraulic fracturing (fracking) has been proved as an effective technique to exploit and increase the production of unconventional resources such as shale gas and shale oil [1,2]. In the process of hydraulic fracturing, the formulation of drilling scheme (e.g., the selection and pumping of fracturing fluid and proppant) usually depends on the in-situ physical properties of reservoirs, in which the fracability of reservoir is often associated with brittleness of reservoir rocks [3,4]. The latter property directly reflects the expected complexity of fractures and the possible level of reservoir stimulation, which are key factors evaluating production potential of reservoirs [5]. There have been previous studies [6–11] that established different indices to measure the brittleness of reservoir rocks, which are based on theoretical [6–9], laboratory experimental [8–10] and statistical [11] analysis, respectively. The related reviews (see Zhang et al. [12] and Mews et al. [13], for example) have systematically described the differences and suitable conditions of these indices. However, both the parameters about the components and the parameters about the physical properties of reservoir rocks are usually derived from laboratory experiments, which are quite different from that derived from in-situ conditions [14,15]. Although there have been experimental studies [16–18] that attempted to restore the in-situ conditions in laboratory, it is still very hard to achieve the goal due to the complexity of multi-scale structures and the heterogeneously in-situ mechanical, thermal and electromagnetic reservoir conditions [19,20]. Theoretically, the intricacy leads to a series of multi-scale scientific issues under the new concept of "mechano-energetics" [21]. For example, the challenge in the formulation of elastic problem with initial stress field and the uniqueness of their solutions [22,23]. Therefore, it is of particularly significance to obtain the in-situ properties of reservoir rocks from the construction site to accurately guide the design of the developing scheme.

At the same time, a lot of evidence [24,25] points to the conclusion that hydraulic fracturing could induce the activity of pre-existed natural faults and further lead to injection-induced earthquakes. Therefore, estimations of reservoir fracture events and hydraulic fracture propagation are essential to avoid the relevant hazards. However, current methods to estimate the propagation of hydraulic fractures are mostly circumstantial evidence and

* Corresponding author. State Key Laboratory of Nonlinear Mechanics, Institute of Mechanics, Chinese Academy of Sciences, Beijing, 100190, China.
E-mail address: yzhao@imech.ac.cn (Y.-P. Zhao).

https://doi.org/10.1016/j.energy.2022.124043
0360-5442/

usually need post-fracturing analysis [59]. They are generally combined with not only far field technologies such as micro-seismic monitoring [26] and tiltmeter measurement [27] but also near wellbore technologies such as radioactive tracer and temperature log [28,29]. A real-time estimation of fracturing situation will be of significant benefit to the evaluation and adjustment of drilling scheme.

The above-mentioned engineering requirements put forward a high demand for the acquisition of in-situ field data. In the process of hydraulic fracturing, fracturing curves (also called pumping curves) are the most direct and firsthand field data, whether it is in the hydraulic test stage or the main hydraulic fracturing stage [1,4]. They provide abundant information [60] on not only the pumping details but also the physical properties of reservoirs. Researchers have carried out a series of theoretical and numerical studies on featured points and featured segments of fracturing curves, including analysis of breakouts pressure and closure pressure [3,4], as well as declination trend analysis based on G-function [30,31]. A lot of essential information, such as in-situ crustal stress value and post-fracking fracture network evaluations, is extracted from the fracturing curves [32,33]. Nevertheless, there is still lots of information hidden in the curves and needs to be revealed, for instance, in-situ brittleness and real-time fracture situations during the fracking process.

In this passage, we focus on the combination of the newly proposed brittleness index [34] and the fracturing curve and aim to propose a fracturing-curve based in-situ brittleness index. With the analysis of fracturing curves data, the Ashby plot is used to show the differences between the in-situ brittleness and the laboratory derived brittleness of reservoir rocks. Fig. 1 shows the basic idea of reservoir evaluation through fracturing curves. Furthermore, with the collaborative study of fracturing curve and micro-seismic data, we intend to reveal the relationship between the fluctuation of fracturing curves before pumping proppants and the fracture behavior of reservoir rocks, as well as seek for a fracturing-curve based way to timely evaluate the fracture propagation. These will provide a guidance on real-time evaluation of fracturing situation and a more accurate design of fracturing scheme before the fracturing process.

2. Materials and methods

2.1. Fracturing curves and micro-seismic data

The analysis of this research is based on the fracturing curve data and micro-seismic data derived from a shale well located in the Woodford Shale in Hughes County, Oklahoma [35]. This horizontal well was fractured with multistage technology, with 5 approximately horizontal stages varying from a depth of 2400 m–2240 m. During the fracturing processes, the fracturing curves of stage I to stage V as well as the surface and downhole micro-seismic data of stage II to stage V were recorded.

The fracturing curves consist of four curves, which are the tubing pressure, the slurry rate, the slurry proppant concentration and the proppant pumped for stage, respectively. As shown in Fig. 2, the fracturing-curves plot of stage I can be divided into 4 main sections: the test section (section I), the non-proppant

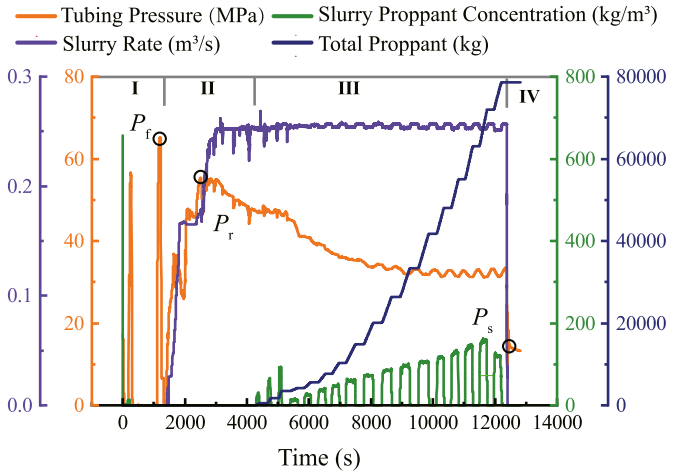

Fig. 2. Stage I hydraulic fracturing curves of investigated Woodford Shale well (modified after Neuhaus [35]). I, II, III and IV represent the fracturing sections. P_f, P_r and P_s are breakdown pressure, refracture pressure and shut-in pressure, respectively.

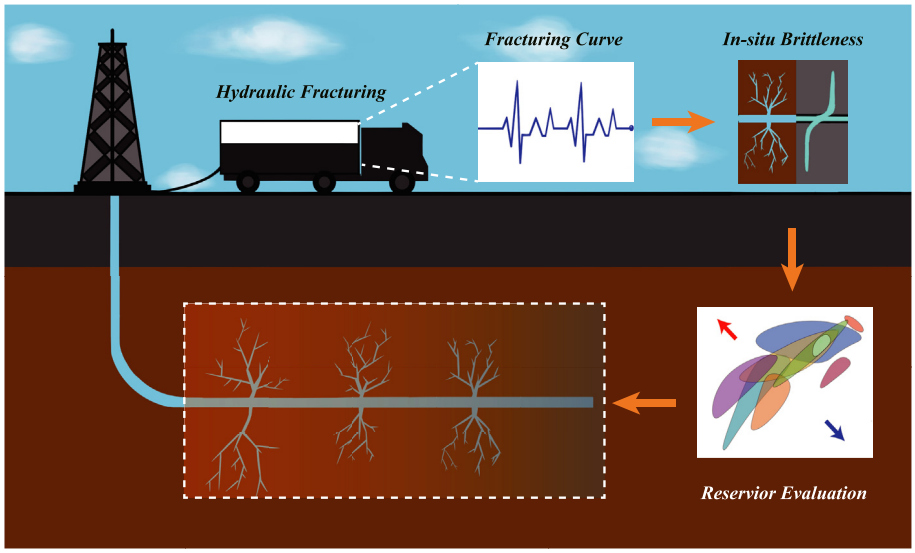

Fig. 1. Schematic of the "diagnosis" of reservoir situations with fracturing curve.

fracturing section (section II), the proppant fracturing section (section III) and the shut-in section (section IV). Section II and section III are the main sections where fractures propagate and micro-seismic events occur. The two sections directly determine the fracture complexity of reservoirs after fracturing. However, in section III, the injection of proppants brings more artificial fluctuations to the tubing curve and makes the real-time calculation of downhole pressure more difficult [36]. Therefore, in this study, section II where the reservoirs are fractured by water is mainly considered. The meaningful key points in the tubing pressure curve are pointed out in Fig. 2, which are breakdown pressure P_f, refracture pressure P_r and shut-in pressure P_s, respectively.

2.2. Ashby plot

Based on the analysis on the typical pressures, we aim at deriving in-situ brittleness of reservoir rocks, which is related to the toughness and strength of rocks (see Section 3 for details). Here we use the Ashby plot as an expression form to clearly express and evaluate the in-situ brittleness of reservoir rocks. Ashby plots were first proposed by Ashby [37] and quickly became efficient standards to select engineering materials (e.g., metals, polymers, ceramics and glasses) for specific applications [38,39]. Recently, the Ashby plots were applied to the evaluation of geomaterials such as rocks for the first time [34]. They are plotted in two or three dimensions that are fundamental properties of materials. Usually there is an additional axis in Ashby plots, which have definite physical meaning (such as deformation and size of an area) and is usually an operational combination of the basic dimensional parameters, to describe the concerned value in specific engineering applications. In this work, we use fracture toughness and tensile strength of rocks as the vertical and horizontal axes, respectively, and the in-situ brittleness is represented as the inclined contour, which is the third and physically meaningful axis.

3. Theory

As stated in Section 1, the samples used in laboratory experiments are out of in-situ conditions (e.g., mechanical and thermal conditions), which are impossible to completely restore in laboratory conditions due to the complexity and the heterogeneity of the in-situ situations. Therefore, we aim at extracting parameters through in-situ data, especially the fracturing curve data. Here we take the brittleness index derived from the size of the process zone [34].

$$B = \sigma_t \Big/ K_{IC} \sim r_p^{-1/2}, \tag{1}$$

where σ_t is the tensile strength, K_{IC} is the fracture toughness. The brittleness index B is inversely proportional to $\sqrt{r_p}$, where r_p is the radius of the process zone [40] ahead of the fracture tip.

The key problem in applying this index to the field is deriving the in-situ tensile strength and fracture toughness. Hence, the calculation of the in-situ tensile strength of rocks is based on the tubing pressures

$$\sigma_t = P_f - P_r, \tag{2}$$

which supposes that the reservoir rocks near wellbore are intact without pre-existing cracks before reaching the breakdown pressure. Equation (2) indicates the breakdown process has released the strength constraint of the reservoir rocks. After that, due to the pre-existence of cracks caused by breakdown pressure, the hydraulic fractures propagate in a toughness dominate regime after the refracture process [41,42], overcoming crustal stress and fracture resistance. Thus, the in-situ fracture toughness can be derived from the refracture process or steady propagation process, which can be calculated by the theory of linear elastic fracture mechanics [43,44].

$$K_{IC} = (P' - \sigma_d)\sqrt{\pi l}, \tag{3}$$

where l is the half-length of hydraulic fracture, σ_d is the confining stress, P' is the downhole pressure. The downhole pressure can be calculated based on the tubing pressure by taking the liquid gravity and flow friction induced pressure drop [36]. Here we take the results of the calculation by Neuhaus [35]. In the calculation of the confining stress, crack length must be taken into consideration because the confining stresses that resist fracture propagation are different near the circular wellbore and far from wellbore. That is, under the assumption that the horizontal wellbore is along the direction of the minimum crustal stress σ_h, crack initiates perpendicular to the minimum confining stress $\sigma_d = 3\sigma_H - \sigma_V$, where σ_H and σ_V are the maximum horizontal principal stress and the vertical principal stress, respectively. In addition, when it is far from the wellbore, crack propagates perpendicular to the minimum horizontal crustal stress $\sigma_d = \sigma_h$ [3,32], When considering the situation that the crack initiates near the wellbore, the crack half-length can be taken as $l = r + a$ [43], where r is the wellbore radius and a is the perforation length.

Therefore, in the initiation stage of the refracture process, Eq. (1) can be expressed as

$$B = \frac{\sigma_t}{K_{IC}} = \frac{P_f - P_r}{(P'_r - 3\sigma_H + \sigma_V)\sqrt{\pi(r+a)}}, \tag{4}$$

in which P'_r is the downhole refracture pressure and the main parameters are all derived from the in-situ situations. Thus, the brittleness derived through Eq. (4) is an in-situ brittleness index. Particularly, Eqs. (2) and (3) are widely used in in-situ stress measurement and all the parameters can be derived through a hydraulic fracturing test, which indicates that the in-situ brittleness can also be derived in a hydraulic fracturing experiment for in-situ stress measurement. Though a recent study [45] showed that the toughness calculated by Eq. (3) may be not accurate when the viscosity of fracturing fluid is high, because it ignores the compliance in the flow of fracturing fluid, it is still effective for low viscosity fluids such as water.

4. Results and discussion

4.1. In-situ brittleness derived from the fracturing curve

The in-situ brittleness of the Woodford Shale well is calculated through Eq. (4) with the following approximations: 1), the initial crack half-length is calculated by the radius of wellbore, where the perforation length is assumed to be small as compared to the wellbore radius; 2), by assuming the variation between the maximum and the minimum horizontal stress is not large, meaning the reservoir is under a biaxial state of stress, the value of σ_H is taken by the value of σ_h, which equals to the shut-in downhole pressure [32]; 3), the vertical principal stress is then calculated by the gravity of overlying rocks by taking the density as 2500 kg/m^3 [46].

Fig. 3 plots the fracture toughness against the tensile strength of rocks, in which the inclined dashed lines are the contour of brittleness index. Rocks towards the top left corner are more ductile while rocks towards the bottom right corner are more brittle. The in-situ brittleness of the Woodford Shale well is compared with those derived from laboratory experiments in Ashby plot [34]. As

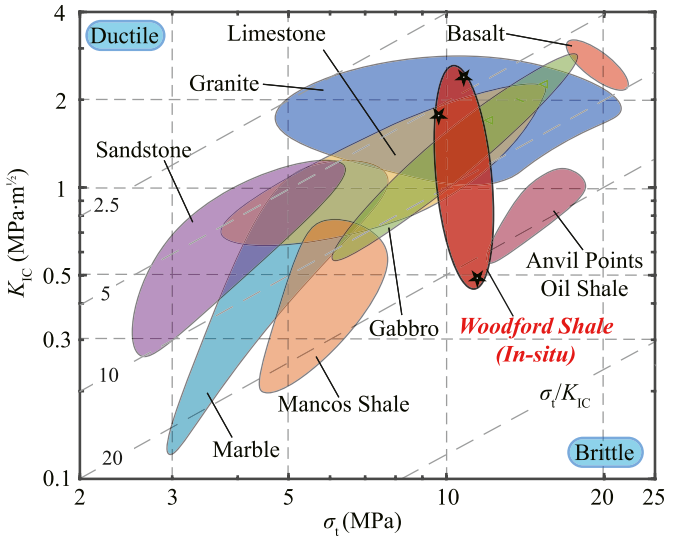

Fig. 3. Brittleness of rocks. The in-situ values of fracture toughness K_{IC} , tensile strength σ_t , and brittleness $B = \sigma_t/K_{IC}$ of investigated Woodford Shale are respectively plotted with contrast to the laboratory experimental results of Sandstone [47–49], Granite [47–49], Marble [48–50], Gabbro [48], Limestone [47,48,51], Basalt [48], Mancos Shale [52] and Anvil Points Oil Shale [48].

shown in Fig. 3, when compared with the laboratory-derived data from Mancos Shale, both the in-situ toughness and the in-situ tensile strength is higher in the field situation of Woodford Shale, while the variation in toughness is more significant. The in-situ toughness is also higher than the toughness of other recorded Woodford Shale samples tested in laboratory conditions, which is 0.38–0.76 MPa m$^{1/2}$ [53]. Note that in the calculation of the in-situ toughness, the above approximations make the calculated toughness a little smaller than the actual value, which indicates that the difference of brittleness could be even larger. The large difference between the in-situ and the laboratory derived brittleness would make it inaccurate to formulate fracturing schemes based on laboratory experimental brittleness. That is, the in-situ value of brittleness will significantly promote the accuracy of the fracturing scheme formulation.

Reservoir rocks are in an extreme field environment where the temperature and the confining stress is much higher than that on earth's surface, which is difficult to reproduce in laboratory [16]. This also leads to the large difference between the in-situ values and the laboratory derived values of physical quantities in Fig. 3. Previous studies also support this point of view. For example, a 20 MPa confining stress can lead to a maximum of 6 times variation in fracture toughness of rocks according to experimental facts (see Gehne et al. [54], for example). A 100 °C temperature increase can make the maximum toughness of rocks two times of its original value [55]. In general, confining stress and temperature is proportional to the depth of the reservoir. This also gives reason to the phenomenon that the complex fracture network is difficult to form with the increase of reservoir depth.

4.2. Scaling of the declining curve in the non-proppant fracturing section

In the non-proppant fracturing section, as shown in Fig. 2, the tubing pressure curve first experiences a continuous rise and then declines rapidly after reaching the maximum value, during which the declination of the pressure reflects the propagation of hydraulic fractures. As an important signal in the study of hydraulic fracturing, the scaling law of the pressure curve indicates the energy dissipation mechanism during the initiation and propagation of hydraulic fractures [41]. In this study, we investigated the scaling law between downhole net pressure and time of stage I, III, IV and V, in which the downhole net pressure is defined as the difference between the downhole pressure and the shut-in pressure (the minimum in-situ principal stress). The data of stage II is not taken into consideration in this subsection and the subsection 4.3 because of the two obvious leak-off segments. The method to measure the scaling law of pressure is the linear regression of log-log formed pressure-time curve. In this method, the scaling law is derived by the slope of the fitted pressure, with a confidence level presented by the coefficient of determination. The least squares method [56] is used for linear regression.

As shown in Fig. 4, the non-proppant sections in all 4 stages behave strongly linear declinations in log-log graphs, in which the scaling laws are between −1/6 and −1/2. The range of the scaling law is a little wider than the theoretical scaling laws predicted by modeling solids and fluids by linear elastic fracture mechanics and lubrication theory, respectively, which is between −1/5 (in toughness-dominated regime) and −1/3 (in viscosity-dominated regime). See Detournay [41] and Garagash [40] for the details of theoretical derivation, for example.

The difference between the results derived from theoretical models and that from field data is mainly due to the assumptions and simplifications in the modeling process. On the one hand, in the theoretical models, only single straightly propagating hydraulic fractures are considered, while there are multiple fractures propagate concurrently [57] and may experience deflections [58] in field conditions. On the other hand, the field reservoir rocks are not totally isotropic and homogeneous, and usually have unpredictable natural fractures and faults. The latter will not only lead to the variation of scaling laws, but also bring in fluctuations on tubing curves. These can significantly affect the propagating situation of the hydraulic fractures. From another point of view, the in-situ fracture propagating situation in reservoirs, which determines the level of reservoir stimulation, can also be inferred from the analysis on fracturing curve fluctuations.

4.3. Fluctuation analysis of the fracturing curve declination

Based on the scaling law analysis in subsection 4.2, we combined fluctuation analysis with the surface and downhole microseismic records, which indicate the happening of fracture events, to find out the relationship between the fluctuation of tubing curves and the in-situ fracture events. In the analysis, stages III, IV and V are taken into consideration, because the lack of the microseismic data at stage I. The pressure data used in the analysis are residual pressure (the difference between real downhole pressure and fitted pressure) and the 1st derivative of the residual pressure. By considering the fitted pressure as the ideal fracturing curve where the hydraulic fractures propagate uniformly and steadily without any crosses with natural fractures, the residual pressure represents the deviation between ideal conditions and field conditions. The deviation is expressed as the fluctuation of residual pressure and its first derivative.

There are multiple natural and artificial factors that can lead to the fluctuation. One obvious factor is the heterogeneity of the reservoir such as the anisotropy of rocks and the effect of natural fractures. For example, the occurrence of weak face may lead to sudden fracture events and the consequent fluid filling beyond normal fracture propagation. This is reflected in the fracturing treatment curves as the instantaneous pressure drops in Figs. 4 and 5. Likewise, when the tips of hydraulic fractures meet the hard-to-propagate areas caused by the heterogeneity of reservoir rocks, the sudden increase in fracture toughness may cause crack propagation

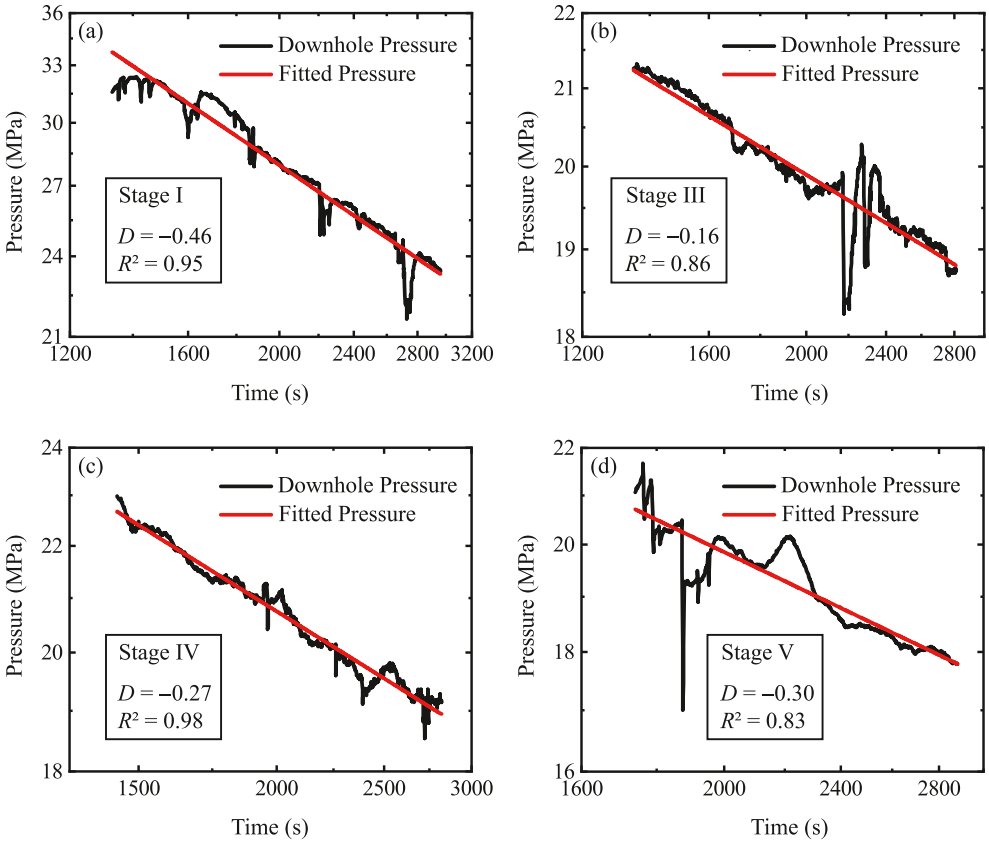

Fig. 4. Scaling of the downhole pressure in non-proppant section. Data belonging to (a) stage I, (b) stage III, (c) stage IV and (d) stage V is plotted in a log-log form. D is the slope of the fitted pressure and R^2 is the coefficient of determination.

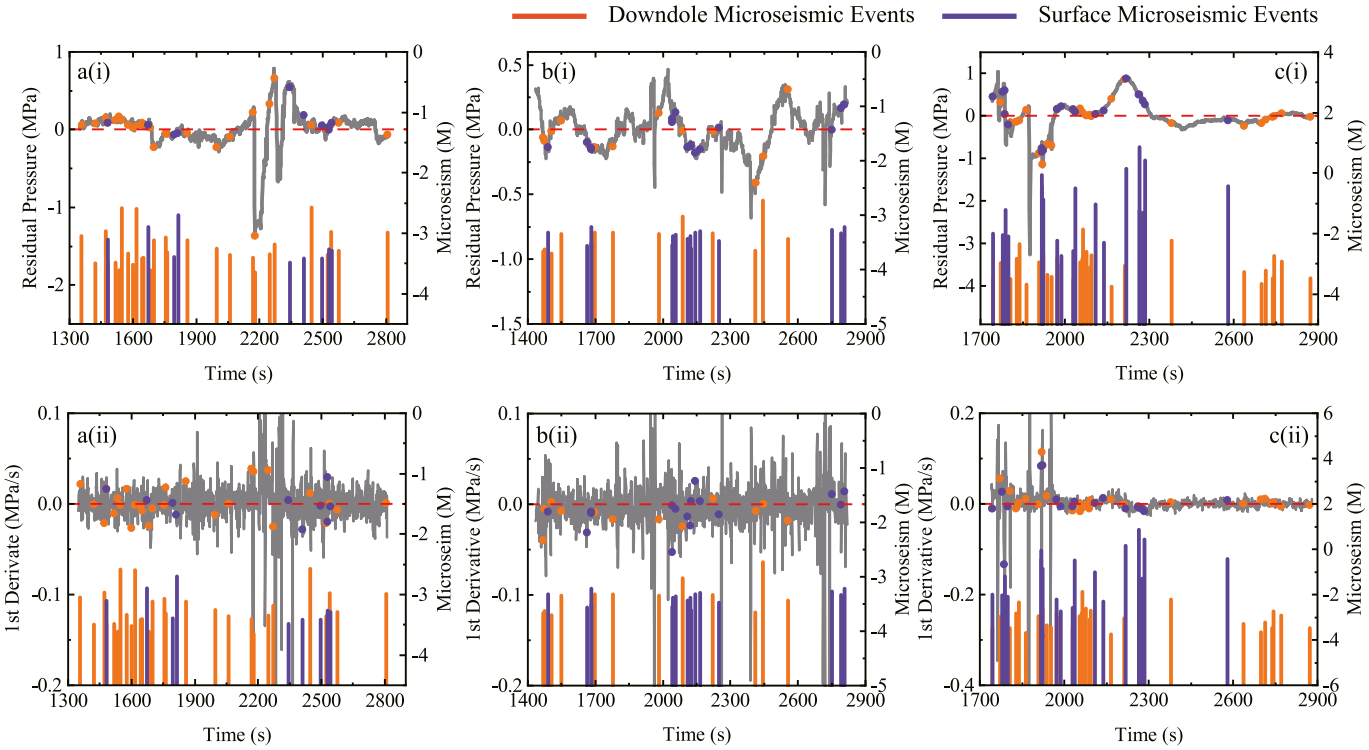

Fig. 5. Relationship between fracturing curve fluctuation and micro-seismic events. Micro-seismic data is in conjunction with the (i) residual pressure and its (ii) 1st derivative of a) stage III, b) stage IV and c) stage V, where M refers to the magnitude of the micro-seismic events.

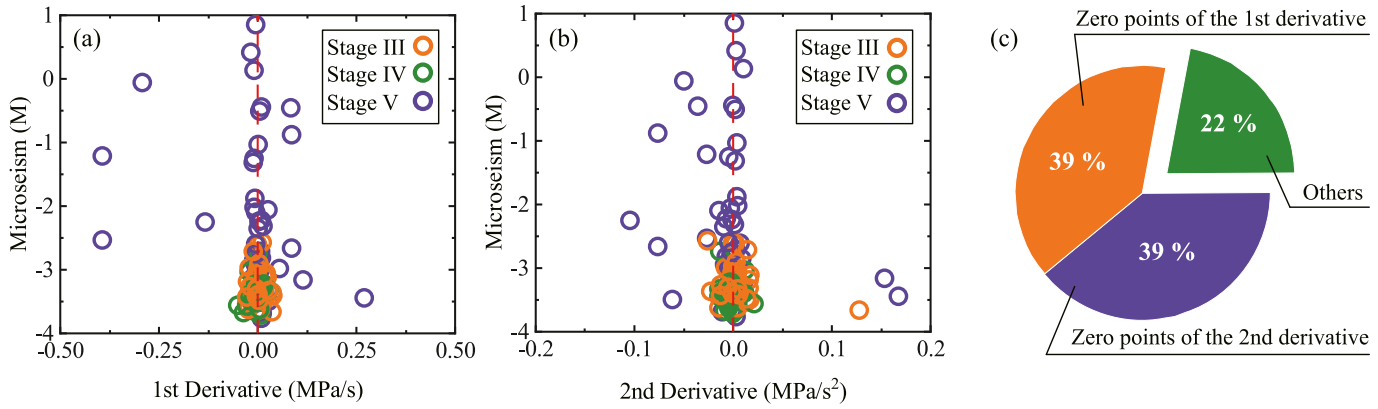

Fig. 6. Statistics at the points of the micro-seismic events. Pictures show the statistics of the magnitude (M) of the micro-seismic events versus (a) the 1st derivative and (b) the 2nd derivative of the residual pressure curves. (c) shows a total distribution of the micro-seismic events.

to stop. At the same time, fluid injection will lead to a continuous rise in pressure until the pressure reaching a critical value to drive the hydraulic fractures to repropagate, which is usually followed by another drop on the fracturing curve.

The alternation of trough and peak pressures greatly reflects the fracturing process of the reservoir. This fact was ignored in previous studies, in which the micro-seismic data could only be used for an overall evaluation of reservoir stimulation level. Here, the real-time micro-seismic data helps us reproduce the details of the hydraulic fracturing process. As shown in Fig. 5, both surface and downhole micro-seismic events are more likely to occur at peaks and troughs. However, there are no direct associations between the absolute value of residual pressure and the degree of micro-seismic event, especially in some huge troughs, where the degrees of micro-seismic events are not higher than that at other points. We hold the opinion that this phenomenon occurs when propagating hydraulic fractures meet large natural fractures, which leads to the rapid drop in pressure. The fractures will further propagate when the natural fractures are filled up and the pressure reaches a critical value. This view is also supported by the micro-seismic events at the post-trough climbing stage and the subsequent peaks of the pressure residual curve in Fig. 5a(i) and 5b(i). This further leads to the fact that fracture events not only occur at the points where the 1st derivative of residual pressure is zero (corresponding to the extreme points of the residual pressure), but also occur at the extreme points of the 1st derivative of the residual pressure (corresponding to where the residuals change the fastest), as shown in Fig. 5a(ii), 5b(ii) and 5c(ii).

It is important to note that the magnitude of either surface or downhole micro-seismic data is not directly resulting in the fluctuation range of the fracturing curve. In other words, the amount of energy released during a hydraulic fracturing induced micro-seismic does not directly results in the change in pressure of the injected fluid.

Further statistical results of the data in Fig. 5 indicates that in the non-proppant fracturing section of the investigated Woodford Shale well, most micro-seismic events happen at the zero points of the 1st and the 2nd derivatives of residual pressure (where the residual pressure reaches its extreme values and where residual pressure changes the fastest, respectively), as shown in Fig. 6(a) and (b). Specifically, the micro-seismic events happen at the extreme points of the residual pressure (where the 1st derivates are zero) and the 1st derivate of the residual pressure (where the 2nd derivates are zero) are of 39% and 39%, respectively. In other words, most (78%) of the fracture events can be predicted in real time, at the extreme points of the residual pressure and the 1st derivative points. Therefore, the fluctuation of tubing curve can be an evaluation criterion of the fracture probability and reservoir stimulation level.

The statistical results indicate that the fluctuation of fracturing curve is closely related to the fracture behavior of reservoir rocks in the investigated shale well. Based on this phenomenon, we suggest an evaluation method on reservoir fractures, in which the fracture events are expressed by the amount and the frequency of micro-seismic record. The fluctuation of the curve is expressed by the variance S^2 and the standard deviation S after fitting, which can be

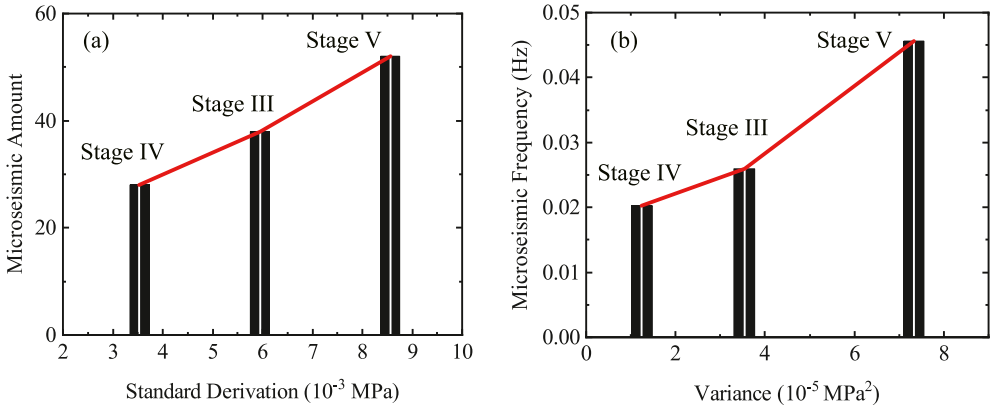

Fig. 7. Fluctuation of fracturing curves reflects the fracture events in reservoir. (a) The total amount of micro-seismic events is positively related to the standard deviation of the pressure curve. The frequency of the micro-seismic events is positively related to the variance of the pressure curve.

expressed as

$$S = \sqrt{S^2} = \sqrt{\frac{1}{n-1}\sum_{i=1}^{n}\left(P^i - P^i_{\text{fit}}\right)}, i = 1, 2, \cdots n \tag{5}$$

where n is the number of the recorded pressure data, and P_{fit} is the fitted pressure. In probability theory and statistics, the variance and the standard deviation are usually used to measure the dispersion, which represents how far a set of numbers is spread out from their average value. Here we use these two quantities to measure the fluctuation degree of the fracturing curve. As shown in Fig. 7(a) and (b), the fluctuation of fracturing curve is strongly corelated with the fracture events, in which standard deviation is positively related to the amount of the fracture event [Fig. 7(a)] and the variance is positively related to the frequency of the fracture events [Fig. 7(b)]. Therefore, the reservoir stimulation efficiency can be inferred by the fluctuation of fracturing curve, especially the variance. This can provide a quick and effective way to evaluate the stimulation situation in the real-time field treatments of hydraulic fracturing.

5. Conclusions

We have established a field method to evaluate the in-situ brittleness and real-time fracturing characteristics of reservoirs. Different from traditional methods that are based on laboratory experiments, all the data in this method is from the field reservoirs under real triaxial stress and temperature conditions. An entirely field-data-based brittleness is proposed to make an accurate evaluation of reservoir fracability. The fracturing curve and the real-time micro-seismic data are combined, for the first time, to make a real-time analysis of the reservoir fracturing characteristics. We show that the in-situ brittleness of reservoir rocks under field conditions is lower than traditional laboratory derived values. This gives a scientific explanation of the fact that fracture network is hard to form in deep reservoirs. It is shown that in the investigated Woodford Shale well, 78% of the micro-seismic events can be predicted in real time through the fluctuation of fracturing curves.

Finally, it is pointed out that this work provides an accurate evaluation method of the in-situ brittleness for the energy field to make precise formulation of fracturing scheme. Fracturing curve fluctuation analysis can be further used in the exploitation field to give a real-time recognition of fracturing characteristics and a guide for optimization of scheme during construction. Furthermore, the scaling law of fracturing curve is found to have a wider range than current theoretical prediction. This provides a direction for more accurate theoretical models to better understand the mechanism of hydraulic fracturing.

Credit author statement

Fuqiang Sun: Methodology, Analysis, Writing - original draft, Editing. **Shuheng Du:** Methodology, Analysis, Writing - review & editing. **Ya-Pu Zhao:** Methodology, Writing - review & editing, Supervision, Project administration.

Declaration of competing interest

The authors declare that they have no known competing financial interests or personal relationships that could have appeared to influence the work reported in this paper.

Acknowledgements

This work was jointly supported by National Natural Science Foundation of China (NSFC, Grant No. 12032019, 41902132, 11872363), PetroChina Innovation Foundation (Grant No.2019D-5007-0214), Chinese Academy of Sciences (CAS) through the CAS Key Research Program of Frontier Sciences (Grant No. QYZDJ-SSW-JSC019) and the CAS Strategic Priority Research Program (Grant No. XDB22040401).

References

[1] Belyadi H, Fathi E, Belyadi F. Hydraulic fracturing in unconventional reservoirs: theories, operations, and economic analysis. second ed. Cambridge: Gulf Professional Publishing; 2019.
[2] Hughes JD. A reality check on the shale revolution. Nature 2013;494:307–8.
[3] Zoback MD. Reservoir geomechanics. Cambridge: Cambridge University Press; 2010.
[4] Yew CH, Weng X. Mechanics of hydraulic fracturing. second ed. Waltham: Gulf Professional Publishing; 2014.
[5] Grieser WV, Bray JM. Identification of production potential in unconventional reservoirs. In: SPE Production and Operations Symposium. Oklahoma; 2007.
[6] Goodway B, Perez M, Varsek J, Abaco C. Seismic petrophysics and isotropic-anisotropic avo methods for unconventional gas exploration. Lead Edge 2010;29:1500–8.
[7] Hucka V, Das B. Brittleness determination of rocks by different methods. Int J Rock Mech Min Geomech Abstr 1974;11:389–92.
[8] Martin CD. Seventeenth canadian geotechnical colloquium: the effect of cohesion loss and stress path on brittle rock strength. Can Geotech J 1997;34:698–725.
[9] Hajiabdolmajid V, Kaiser P, Martin CD. Mobilised strength components in brittle failure of rock. Geotechnique 2003;53:327–36.
[10] Jarvie DM, Hill RJ, Ruble TE, Pollastro RM. Unconventional shale-gas systems: the mississippian barnett shale of north-central Texas as one model for thermogenic shale-gas assessment. AAPG Bull 2007;91:475–99.
[11] Rickman R, Mullen MJ, Petre JE, Grieser WV, Kundert D. A practical use of shale petrophysics for stimulation design optimization: all shale plays are not clones of the barnett shale. In: Proceedings of the SPE Annual Technical Conference and Exhibition. Denver; 2008.
[12] Zhang D, Ranjith PG, Perera MSA. The brittleness indices used in rock mechanics and their application in shale hydraulic fracturing: a review. J Petrol Sci Eng 2016;143:158–70.
[13] Mews KS, Alhubail MM, Barati RG. A review of brittleness index correlations for unconventional tight and ultra-tight reservoirs. Geosci 2019;9:319.
[14] Von Karman T. Festigkeitsversuche unter allseitigem drunk. Z Ver Deu Ing 1911;55:1749.
[15] Haimson B. True triaxial stresses and the brittle fracture of rock. Pure Appl Geophys 2006;163:1101–30.
[16] Lin K, Huang X, Zhao Y-P. Combining image recognition and simulation to reproduce the adsorption/desorption behaviors of shale gas. Energy Fuel 2019;34:258–69.
[17] Mahzari P, Mitchell TM, Jones AP, Oelkers EH, Striolo A, Iacoviello F, et al. Novel laboratory investigation of huff-n-puff gas injection for shale oils under realistic reservoir conditions. Fuel 2021;284:118950.
[18] Mahzari P, Mitchell TM, Jones AP, Westacott D, Striolo A. Direct gas-in-place measurements prove much higher production potential than expected for shale formations. Sci Rep 2021;11:10775.
[19] Lin K, Zhao Y-P. Entropy and enthalpy changes during adsorption and displacement of shale gas. Energy 2021;221:119854.
[20] Du S. Profound connotations of parameters on the geometric anisotropy of pores in which oil store and flow: a new detailed case study which aimed to dissect, conclude and improve the theoretical meaning and practicability of “umbrella deconstruction” method furtherly. Energy 2020;211:118630.
[21] Zhao Y-P. Physical mechanics investigation into carbon utilization and storage with enhancing shale oil and gas recovery. Sci China Technol Sci 2022;65:490–2.
[22] Gao MN, Zhao YP. Some uniqueness theorems of solutions for the problems of elasticity. SCIENTIA SINICA Physica, Mechanica & Astronomica 2020;50:56–89.
[23] Zhao YP. A course in rational mechanics. Beijing: Science Press; 2020.
[24] Ellsworth WL. Injection-induced earthquakes. Science 2013;341:142–9.
[25] Lei XL, Huang DJ, Su JR, Jiang GM, Wang XL, Wang H, et al. Fault reactivation and earthquakes with magnitudes of up to mw4.7 induced by shale-gas hydraulic fracturing in sichuan basin, China. Sci Rep 2017;7:7971.
[26] Warpinski N. Microseismic monitoring: inside and out. J Petrol Technol 2009;61:80–5.
[27] Wright CA, Davis EJ, Weijers L, Golich GM, Ward JF, Demetrius SL, et al. Downhole tiltmeter fracture mapping: a new tool for directly measuring hydraulic fracture dimensions. In: SPE annual technical conference and exhibition. New Orleans; 1998.
[28] Nelson AW, Eitrheim ES, Knight AW, May D, Mehrhoff MA, Shannon R, et al. Understanding the radioactive ingrowth and decay of naturally occurring radioactive materials in the environment: an analysis of produced fluids from the marcellus shale. Environ Health Perspect 2015;123:689–96.
[29] Wood DA. Gamma-ray log derivative and volatility attributes assist facies

characterization in clastic sedimentary sequences for formulaic and machine learning analysis. Adv Geo-Energy Res. 2022;6:69–85.
[30] Nolte KG. Determination of fracture parameters from fracturing pressure decline. In: SPE annual technical conference and exhibition. Las Vegas; 1979.
[31] Nolte KG. A general analysis of fracturing pressure decline with application to three models. SPE Form Eval 1986;1:571–83.
[32] Zang A, Stephansson O. Stress field of the earth's crust. Dordrecht: Springer; 2009.
[33] Wang H, Elliott B, Sharma M. Pressure decline analysis in fractured horizontal wells: comparison between diagnostic fracture injection test, flowback, and main stage falloff. SPE Drill Complet 2021;36:717–29.
[34] Sun FQ, Zhao YP. Geomaterials evaluation: a new application of ashby plots. Materials 2020;13:2517.
[35] Neuhaus CW. Analysis of surface and downhole microseismic monitoring coupled with hydraulic fracture modeling in the woodford shale. Colorado School of Mines; 2011.
[36] Hannah RR, Harrington LJ, Lance LC. The real-time calculation of accurate bottomhole fracturing pressure from surface measurements using measured pressures as a base. San Francisco: SPE Annual Technical Conference and Exhibition; 1983.
[37] Ashby MF. A first report on deformation-mechanism maps. Acta Metall 1972;20:887–97.
[38] Ritchie RO. The conflicts between strength and toughness. Nat Mater 2011;10:817–22.
[39] Ashby MF. Materials selection in mechanical design. fifth ed. Oxford: Butterworth-Heinemann; 2017.
[40] Garagash DI. Cohesive-zone effects in hydraulic fracture propagation. J Mech Phys Solid 2019;133:103727.
[41] Detournay E. Mechanics of hydraulic fractures. Annu Rev Fluid Mech 2016;48:311–39.
[42] Shen WH, Yang FQ, Zhao YP. Unstable crack growth in hydraulic fracturing: the combined effects of pressure and shear stress for a power-law fluid. Eng Fract Mech 2020;225:106245.
[43] Abou-Sayed AS, Brechtel CE, Clifton RJ. In-situ stress determination by hydrofracturing: a fracture mechanics approach. J Geophys Res 1978;83:2851–62.
[44] Zhao Y-P. Modern continuum mechanics. Beijing: Science Press; 2016.
[45] Gao Y, Detournay E. Fracture toughness interpretation from breakdown pressure. Eng Fract Mech 2021;243:107518.
[46] Mavko G, Mukerji T, Dvorkin J. The rock physics handbook. third ed. Cambridge: Cambridge University Press; 2020.
[47] Bearman RA. The use of the point load test for the rapid estimation of mode I fracture toughness. Int J Rock Mech Min Sci 1999;36:257–63.
[48] Zhang ZX. An empirical relation between mode I fracture toughness and the tensile strength of rock. Int J Rock Mech Min Sci 2002;39:401–6.
[49] Rao Q, Sun Z, Stephansson O, Li C, Stillborg B. Shear fracture (mode II) of brittle rock. Int J Rock Mech Min Sci 2003;40:355–75.
[50] Wang QZ. The flattened brazilian disc specimen used for determining elastic modulus, tensile strength and fracture toughness of brittle rocks: experimental results. Int J Rock Mech Min Sci 2004;41:357–8.
[51] Gunsallus KL, Kulhawy FH. A comparative evaluation of rock strength measures. Int J Rock Mech Min Geomech Abstr 1984;21:233–48.
[52] Chandler MR, Meredith PG, Brantut N, Crawford BR. Fracture toughness anisotropy in shale. J Geophys Res Solid Earth 2016;121:1706–29.
[53] Chen X, Eichhubl P, Olson JE. Effect of water on critical and subcritical fracture properties of woodford shale. J Geophys Res Solid Earth 2017;122:2736–50.
[54] Gehne S, Forbes Inskip ND, Benson PM, Meredith PG, Koor N. Fluid-driven tensile fracture and fracture toughness in nash point shale at elevated pressure. J Geophys Res Solid Earth 2020;125:1–11.
[55] Chandler MR, Meredith PG, Brantut N, Crawford BR. Effect of temperature on the fracture toughness of anisotropic shale and other rocks. Geological Society, London, Special Publications 2017;454:295–303.
[56] Devore JL. Probability and statistics for engineering and the sciences. ninth ed. Boston: Cengage Learning; 2015.
[57] Lecampion B, Desroches J. Simultaneous initiation and growth of multiple radial hydraulic fractures from a horizontal wellbore. J Mech Phys Solid 2015;82:235–58.
[58] Sun FQ, Shen WH, Zhao YP. Deflected trajectory of a single fluid-driven crack under anisotropic in-situ stress. Extreme Mech Lett 2019;29:100483.
[59] Meng M, Chen Z, Liao X, Wang J, Shi L. A well-testing method for parameter evaluation of multiple fractured horizontal wells with non-uniform fractures in shale oil reservoirs. Adv Geo-Energy Res 2020;4(2):187–98.
[60] Moosavi SR, Vaferi B, Wood DA. Auto-detection interpretation model for horizontal oil wells using pressure transient responses. Adv Geo-Energy Res 2020;4(3):305–16.